J. Fluid Mech. (1999), *vol.* 400, *pp.* 355–374. Printed in the United Kingdom

Convergence of a cylindrical liquid shell and the formation of a bore in a rotating fluid

By V. K. KEDRINSKII AND V. V. NIKULIN

M. A. Lavrentyev Institute of Hydrodynamics, Novosibirsk, 630090, Russia

(Received 5 May 1998 and in revised form 15 July 1999)

This paper presents the results of experimental studies of a collapsing cylindrical cavity (the convergence of a liquid shell) in a rotating fluid as well as the formation and propagation of a jump (bore) at the interface. The basic parameters of the liquid shell dynamics for a pulsed one-dimensional load are estimated using the equation of cylindrical cavity pulsation in an unbounded fluid. The theoretical model of a rotationally symmetric hydraulic jump moving along the free surface of a hollow vortex is constructed. The jump is simulated by a discontinuous solution of the equations in the long-wave approximation for tornado-like and hollow vortices. For comparison with the experimental data, basic theoretical results are obtained for flows in a hollow vortex with constant circulation and axial velocity varying along the radius of the rotating liquid shell.

1. Introduction

A number of problems of wave focusing and flow convergence are at present conveniently considered in the one-dimensional cylindrical formulation, which allows a relatively simple experimental realization for study of the flow pattern features and the stability of interfaces. A similar approach is also sometimes used to solve axisymmetric problems, when the method of independent sections permits one to reconstruct a reasonably accurate picture of the process from 'one-dimensional' results. Two characteristic examples can be cited: the collapse of a conical liquid shell under loading by a detonation wave travelling along the cone surface (classical cumulation), and the generation of a conical shock wave in a fluid as a result of a cord (linear) charge explosion with a finite detonation rate. Consideration of the delay in the detonation propagation time and, correspondingly, the start of the process development in each section, allows quite a good estimation of basic features of the axisymmetric flow.

The problems of cumulation have been examined within the framework of thermonuclear fusion programmes as well (Vakhrameev 1995; Zababakhin 1970; Tarzhanov 1995) and very intensively in the studies of destruction mechanisms in lithotripsy systems (Gronig 1989; Sturtevant 1989; Book & Lohner 1989; Takayama 1989; Fujiwara *et al.* 1993; Demmig *et al.* 1993; Hiroe *et al.* 1993; Kuwahara *et al.* 1991; Isuzukawa & Horiuchi 1991), where the case in point is the focusing in liquid media of short shock waves with an intense and relatively prolonged rarefaction phase following a front, and also the formation and collapse of bubble clusters on solid targets.

Recently interest in the problem of shock wave focusing in the gas phase in

spherical bubbles has been rekindled in connection with the modelling of the sonoluminescence mechanism (Gaitan & Crum 1990; Atchley 1993; Crum 1994) – the effect of an ultrashort light-flash generation during the collapse of cavitation bubbles. It is evident that here the shock waves are excited during the cavity-convergence process, whose liquid walls act as a spherical piston. From these standpoints investigations of various approaches to the formation of convergent fluid flows have a principal role.

In the context of the analysis of one of the possible approaches to the modelling of the processes related to thermonuclear fusion, a rather simple technique to create a liquid cylindrical piston (shell) has been proposed and studied experimentally by Kedrinskii & Pigolkin (1964). The basic idea was that a transparent vertical water-filled cylinder closed at the bottom and with a movable cover at the top, was spun around its axis so that an inner cylindrical cavity formed, which was bounded by a rotating liquid shell. Thereafter the cavity was filled with an explosive gas mixture. In studies of the stability and dynamics of the interface of such a rotating shell, the possibility was analysed of cylindrical gas-cavity compression to the temperature of detonation initiation in the gas mixture filling it (as a result of adiabatic compression). The experiments were carried out for two types of pulse loading: along the axis of the rotating cavity and a cylindrically symmetric variant.

In the first case a new unexpected effect was discovered: at the surface of the cavity a stable jump (bore) was formed which propagated with a velocity exceeding that of the piston generating it. In the second case one-dimensional cylindrical flow was achieved and the nature of the cavity convergence as a function of the initial pressure in it could be investigated.

Regarding the bore effect, one may recall hydraulic jumps in open channels which have been considered in a large body of works. At first, the theoretical description of this phenomenon was restricted to the study of potential flows of an ideal fluid in the shallow water approximation, as, for instance, in Whitham (1974). In recent years a model of the jump has appeared which accounts for the vortex character of the motion (Teshukov 1995). The theory of the vortex jump or vortex breakdown for swirling flows in a tube was originally suggested by Benjamin (1962), where the possibility was considered of a finite transition between two conjugate states of a stationary rotationally symmetric flow in a circular tube. It was assumed that in the transition from one state to another, the total head and circulation are conserved on streamlines. It turned out that the integral of axial momentum flux plus pressure force ('flow force') over a section of the tube increased on transition downstream from one state to another. The approach developed by Benjamin (1962), was applied to flow in tubes with the possibility, after the transition, of cavitation zone formation in the central part of the flow (Keller, Egli & Exley 1985). As the cavitation zone formed, it turned out to be possible to satisfy conditions of constancy of both the total head on the streamlines and 'flow force' after the transition from one state to another.

In this paper, the results of experimental studies of a collapsing cylindrical cavity in a rotating fluid are presented, estimations of basic parameters are suggested, based on the notion of the cavity behaviour in an unbounded fluid, and a theoretical model of a rotationally symmetric hydraulic jump moving along the free surface of a hollow vortex is constructed. The jump is modelled by a discontinuous solution of the equations in the long-wave approximation for tornado-like and hollow vortices obtained by Nikulin (1992*a*). The theoretical model of the process can be developed for the vortex flow wherein only the azimuthal vorticity component is non-zero. For

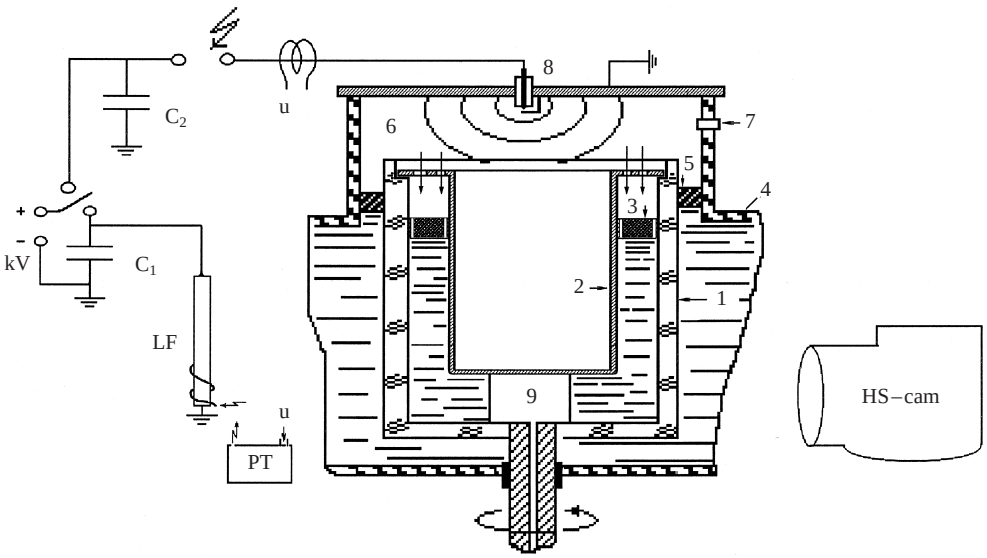

FIGURE 1. Apparatus for investigation of the dynamics of a cylindrical gas cavity in a rotating fluid.

comparison with the experimental data the main theoretical results were obtained for flows in a hollow vortex with constant circulation and at an axial velocity varying along the radius of the rotating liquid shell.

2. One-dimensional flow

2.1. *Cylindrical convergence, experiment*

The layout of the experiment on one-dimensional convergence is presented in figure 1. In a transparent cylindrical tank (1) (its diameter is equal to 100 mm), mounted on the shaft of a motor whose rotation speed could be varied over a sufficiently wide range of values, a cup (2) was inserted, firmly attached to the tank by a special cover with holes. The space between them, bounded from above by an annular piston (3), was filled with a liquid. The shaft had a hole for feeding a reactive gas mixture which could be shut when necessary.

Note that the real shape of the cup 2 is somewhat different from its schematic representation in figure 1. The cup had a gentle expansion in the vicinity of its bottom and its lower edge was smoothly rounded, which prevented flow detachment around it.

Water was used as the working liquid, and the rotational speed of the transparent cylindrical tank in experiments was set to about 30 rev s^{-1}. The distance between the bottom of the cup and the tank bottom measured 25 mm.

The whole system was placed into a chamber (4) with optical windows for observations, which was filled with water. In doing so, not only were conditions for optical recording of the process improved, but together with special collars (5), the rotation of the working cylinder was stabilized as well. The upper part of the chamber was a high-pressure section (6), which was filled with an explosive gas mixture, for example a 50% mixture of acetylene with oxygen, through the hole (7). Note that holes in the inner cup cover ensured that the mixture filled the entire space of section 6 from its

upper face into which a high-voltage spark gap (8) was built, to the annular piston (3). The latter actually became the movable bottom of the high-pressure section.

When the cylinder (1) is rotated, a cylindrical cavity (9) is formed between its bottom and the cup (2) bottom. The size of the cavity is varied by feeding gas through the shaft, by the rotation speed and by the initial pressure of the explosive gas mixture in section 6, which could be set depending on requirements, from units of kPa to 100 kPa. The pistons described (figures 1, 3) were mobile and could be easily displaced by a rotating liquid shell. The two experimental set-ups had a device initiating the detonation of the gas mixture in section 6 in the form of a discharge circuit with a capacitor bank C_2 and high-voltage spark gaps. The synchronization system of the external illumination switches on the Rogowskii belt (u, inductance transducer) and the pulse transformer PT amplifying the signal from the inductance transducer and triggering the flash-lamp LF, on the leads of which the high-voltage capacitor bank C_1 is closed. The high-voltage power supply kV is designed to charge both these capacitor banks. The high-speed camera HS-cam is used for optical recording of the gas-cavity dynamics.

When the gas mixture in section 6 is exploded, the pressure in a shock wave and in detonation products is transferred through the piston 3 to the liquid shell whose rotational speed is kept constant. A typical oscillogram of the pressure in the fluid is presented in figure 2(*b*). In this case the duration of the pulse loading is approximately 2.5 ms and the pressure increases up to 600 kPa in about 1.5 ms. The pressure trace is the same for all cases presented by figure 2(*a*). Notice that initial pressures of gas mixtures in sections 6 and 9, as a rule, are different and the pressure of detonation products in 6 may be controlled by the original composition and quality of the mixture.

The dynamics of the cylindrical cavity in the form of a continuous display of its diameter at the loading mentioned for four different values of the initial pressure p_0 of the gas mixture inside the cavity is shown in figure 2. Scanning is done through a horizontal slit 1 mm wide centrally located in cavity 9 (the other sides of the cavity are closed). The rotating mirror of the camera HS-cam turns the flow pattern in the direction perpendicular to the slit and records on a film the dynamics of the cavity diameter.

It is readily seen that at $p_0 = 60$ kPa (figure 2*a* i) the cavity with the initial radius of $R_0 \approx 3$ cm is compressed approximately six times and the rotation of the compressing liquid shell slightly disturbs the cavity shape. For $p_0 = 20$ kPa (figure 2*a* ii) and the same value of R_0, in the vicinity of the minimum ($d_{min} \approx 5$ mm, the compression ratio is about 12) instability development is observed in the cavity shape as a breaking of flow symmetry which is enhanced by rotating the shell. One can see that the scan is slightly curled. At this instant the external pressure roughly corresponds to the minimum: the cavity is overcompressed to high pressure because of inertial properties of the fluid, which is supported by its subsequent expansion.

At $p_0 = 10$ kPa and $R_0 \approx 3$ cm (figure 2*a* iii), the minimum diameter of the cavity is $d_{min} \approx 3$ mm and the compression ratio is close to 20. In the vicinity of the minimum an evident instability of the cavity shape is observed, manifesting itself in the form of a 'drill coil'. At $p_0 = 6$ kPa and $R_0 \approx 2$ cm (figure 2*a* iv), the compression ratio clearly exceeds its previous value; however it is impossible to find it with a reasonable accuracy: the instability in the vicinity of the minimum radius increases. The minimum occurs at an instant when the external loading has not yet reached its minimum, which explains the large number of small pulsations, constituting the scan structure for $t > 2.75$ ms: the cavity oscillates close to the minimum equilibrium

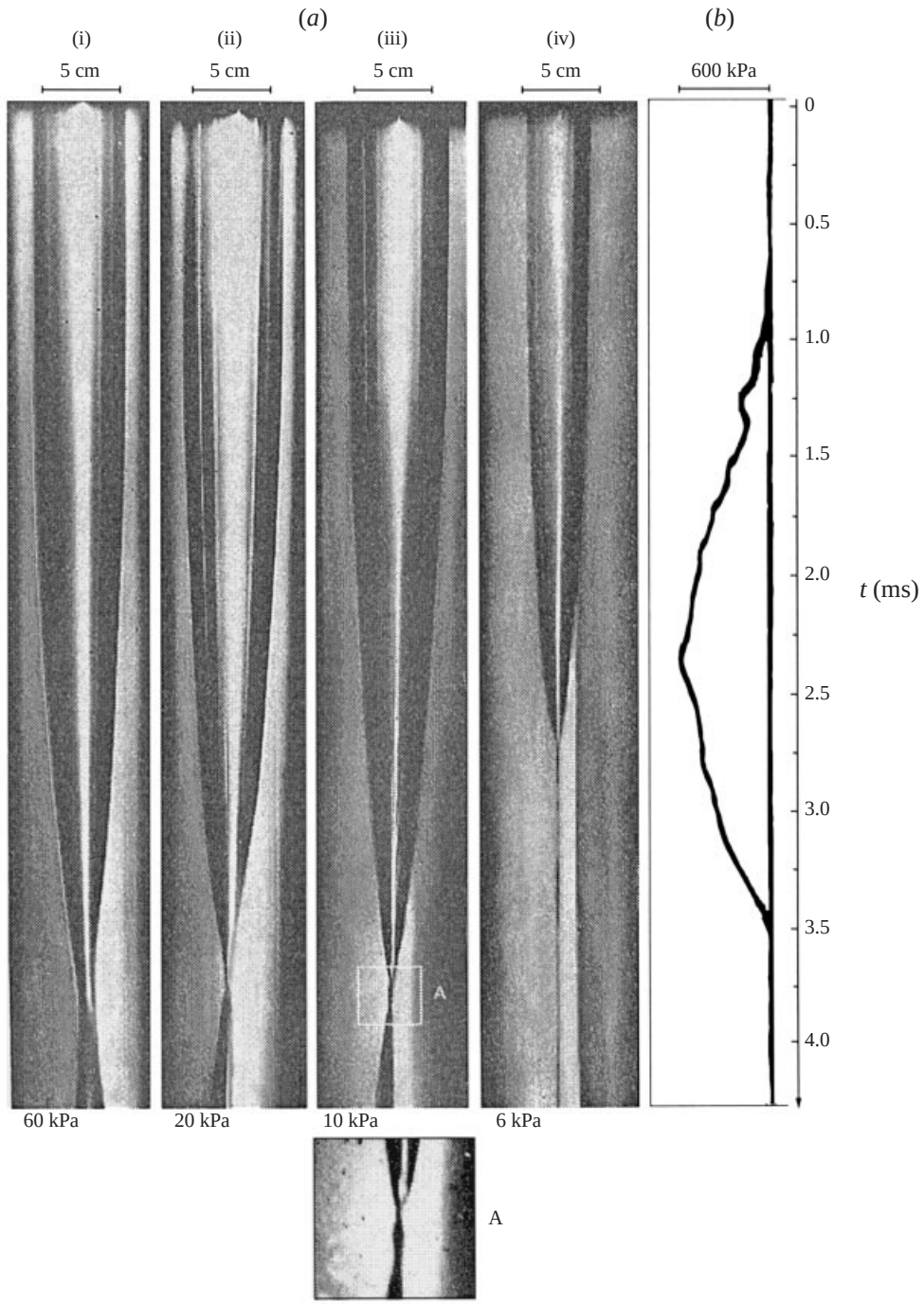

FIGURE 2. (*a*) One-dimensional collapse of a cylindrical cavity at the initial gas pressure of $p_0 = 60$ (i), 20 (ii), 10 (iii) and 6 (iv) kPa (in cavity 9). (*b*) Oscillogram of the pressure.

diameter whose scan takes the form of twisted cord. In conclusion it may be noted that when the compression ratio $R/R_0 \geqslant 10$, the interface instability begins to develop, caused by an imperfection in the cylindrical surface, by the Rayleigh–Taylor instability and by the liquid-shell rotation. This process manifests itself basically in the vicinity

of the minimum cavity diameter. However we can consider that the flow as a whole remains cylindrically symmetric.

2.2. *Theoretical estimations*

The process of cylindrically symmetric convergence of a liquid cavity is modelled within the framework of the problem of cylindrical cavity collapse in an unbounded fluid. Note that when this problem is formulated, difficulties arise even in the simplest case of cylindrical cavity pulsation in an unbounded incompressible fluid. The point is that this problem cannot be precisely formulated as an analogy to the equation of Besant (1859) or Rayleigh (1917): in the cylindrically symmetric case the kinetic energy of the incompressible fluid T_k per unit length has a logarithmic singularity at infinity (at $r \to \infty$ $T_k \to \infty$) :

$$T_k = \pi\rho R^2\dot{R}^2 \ln\frac{r}{R}.$$

A problem with the law of energy conservation arises.

The way round this problem has been found in solving the problem of a linear (or cord) charge explosion in a compressible fluid, based on the invariance of some function $G = r^{n/2}\Omega$ ($n = 0, 1, 2$, where $n = 1$ fits cylindrical symmetry) on the corresponding characteristic curves (Kedrinskii 1971, bib25)

$$\frac{\partial G}{\partial t} + c_0\frac{\partial G}{\partial r} = 0, \tag{2.1}$$

where $\Omega = \omega + v^2/2$ is the kinetic enthalpy, ω is the enthalpy, v is the mass velocity, and c_0 is the sound velocity.

Result (2.1) is obtained as a generalization of the well-known Kirkwood–Bethe approximation, proposed to solve the problem of underwater explosion of spherical charges (Cole 1948). For a potential liquid flow in the acoustic approximation the continuity equation in the one-dimensional case of flat, cylindrical and spherical symmetry ($n = 0, 1, 2$) takes the form

$$\frac{\partial^2\varphi}{\partial r^2} - c_0^{-2}\frac{\partial^2\varphi}{\partial t^2} + \frac{n}{r}\frac{\partial\varphi}{\partial r} = 0,$$

where φ is the velocity potential. If the function $\Phi = r^{n/2}\varphi$ is substituted, this equation can be reduced to the form

$$\frac{\partial^2\Phi}{\partial r^2} - c_0^{-2}\frac{\partial^2\Phi}{\partial t^2} + n(2-n)\frac{\Phi}{4r^2} = 0.$$

Hence it follows, that for $n = 0, 2$ exactly and for $n = 1$ in the asymptotic approximation (the last term is neglected) we obtain the wave equation

$$\frac{\partial^2\Phi}{\partial t^2} - c_0^2\frac{\partial^2\Phi}{\partial r^2} = 0.$$

Considering that in the above functions the pulse conservation equation is written as

$$\frac{\partial\Phi}{\partial t} = G,$$

it is easy to reduce the wave equation to (2.1): let us substitute $\xi = t - r/c_0$, then $\Phi = \Phi(\xi)$, $\Phi_t = G$, $\Phi_{tt} = G_t$, $\Phi_r = -c_0^{-1}\Phi_\xi = -G/c_0$, $\Phi_{rr} = -G_r/c_0$.

Substitution of the function G into equation (2.1) corresponding to the replacement

of partial derivatives for the total ones based on the conservation laws

$$\frac{\mathrm{d}v}{\mathrm{d}t} = -\frac{\partial \omega}{\partial r}, \qquad c_0^{-2}\frac{\mathrm{d}\omega}{\mathrm{d}t} = -\frac{\partial v}{\partial r} - \frac{nv}{r},$$

and the transition to the wall of the cavity ($r = R$, $v|_{r=R} = \mathrm{d}R/\mathrm{d}t$) allow the derivation of a generalized equation describing the pulsation of a one-dimensional cavity (for the plane $n = 0$, spherical symmetry $n = 2$, and, in the asymptotic approximation, for cylindrical symmetries $n = 1$). It takes the form (Kedrinskii 1971, 25)

$$\left(1 - \frac{2\dot{R}}{c_0}\right) R\frac{\mathrm{d}^2R}{\mathrm{d}t^2} + \frac{3}{4}n\left(1 - \frac{4\dot{R}}{3c_0}\right)\left(\frac{\mathrm{d}R}{\mathrm{d}t}\right)^2 = n\frac{\omega}{2} + \left(1 - \frac{\dot{R}}{c_0} + \left(\frac{\dot{R}}{c_0}\right)^2\right)\frac{R}{c_0}\frac{\mathrm{d}\omega}{\mathrm{d}t}. \quad (2.2)$$

Here ω is the enthalpy of the fluid at the wall of the cavity, $\dot{R} = \mathrm{d}R/\mathrm{d}t$. Note that (2.2) for $n = 1$ is approximate, but the approximation in the cylindrical variant is utilized only in deriving the basic equation for the invariant $G = r^{n/2}\Omega$; under other transformations only exact conservation laws are used. The answer to the question of how well this approximation allows one to describe the real process of the dynamics of the cylindrical cavity can be provided experimentally. A comparison of the experimental data on the dynamics of the cavity in exploding linear charges and the calculation results showed (Kedrinskii & Kuzavov 1977) that the basic parameters of the process (the maximum radius of the explosive cavity and its pulsation period) agree well with a good accuracy. In addition, from the analysis of the spherical cavity dynamics, it is well known that the pulsation period T practically does not depend on the compressibility of the fluid and on the gas content of the cavity (for a large compression ratio).

Equation (2.2) has no special features and it is clear that none can arise in passing to the incompressible limit. Let us use our knowledge of the cylindrical variant and proceed to the limit of incompressible fluid in (2.2) ($c_0 \to \infty$, $\omega \to (p_R - p_\infty)/\rho_0$). Then for the cylindrical cavity ($n = 1$) and incompressible fluid we obtain the equation (Kedrinskii 1971)

$$R\frac{\mathrm{d}^2R}{\mathrm{d}t^2} + \frac{3}{4}\left(\frac{\mathrm{d}R}{\mathrm{d}t}\right)^2 = \frac{p_R - p_\infty}{2\rho_0},$$

or in dimensionless form

$$yy_{\tau\tau} + \tfrac{3}{4}y_\tau^2 = \tfrac{1}{2}(\bar{p}y^{-2\gamma} - 1). \quad (2.3)$$

Here the index τ denotes the corresponding derivative, $y = R/R_0$, $\tau = t(p_\infty/\rho_0)^{(1/2)}R_0^{-1}$, $\bar{p} = p_0/p_\infty$; the subscript '0' is assigned to the initial values of the corresponding parameters. It is suggested that the cavity pressure p_R varies by the adiabatic law.

One can use what is known for a spherical cavity (Cole 1948) to find the pulsation period $T_{cyl,*}$ as twice the collapse time of a cylindrical cavity. Let us write (2.3) for an empty cavity, multiply both sides by $y^{1/2}$ and rearrange it in the form

$$\frac{\mathrm{d}}{\mathrm{d}y}(y^{3/2}y_\tau^2) = -y^{1/2}.$$

After a simple manipulation we obtain

$$\tau_{cyl,*} = -\int_1^0 \frac{\mathrm{d}y}{(\frac{2}{3}(y^{-3/2} - 1))^{1/2}} = 0.817F\left(\tfrac{1}{2}, \tfrac{7}{6}, \tfrac{13}{6}, 1\right) \approx 1.49.$$

Here $F(\alpha, \beta, \gamma, z)$ is the Gauss hypergeometric function. In dimensional form

$$t_{cyl,*} \approx 1.49 R_{max} \left(\frac{\rho_0}{p_\infty} \right)^{1/2}, \qquad T_{cyl,*} = 2t_{cyl,*}. \tag{2.4}$$

Experimental verification of the formula obtained for the pulsation period of the cylindrical cavity (the time interval between the shock-wave front and pressure peak of the first pulsation) has been carried out on cord charges of explosives (Kedrinskii 1976). The comparison shows that the agreement of data is quite satisfactory.

By the way, one can set the problem of the dynamics of a cylindrical cavity in the half-space of incompressible liquid and derive the corresponding equation without the features mentioned above. This fits naturally with actual experimental conditions. However, according to the resulting equation, the cavity dynamics proves to be an essential function of the depth h as $\ln(h/R_0)$, which is inconsistent with the experimental data.

Note that the generation of cylindrical convergence using the explosion method is particularly efficient when we are dealing with the necessity of investigating the collapse of a liquid shell into vacuum. Such a system can be created by the explosion of a cylindrical charge of a stoichiometric gas mixture of hydrogen with oxygen, for instance, in the formulation with a rotating fluid. The steam produced from the detonation of such a mixture will condense during the expansion stage and the subsequent cavity-convergence process will not be limited by a 'gas damper'.

Now we can try to use the expression (2.4), derived for an unbounded fluid, to estimate the collapse time of a cylindrical shell in a rotating fluid. Experimental data presented in figure 2 show that cavities with initial radii $R_0 \approx 3\,\text{cm}$ at $p_\infty \approx 600\,\text{kPa}$ reach the minimum in $t_{cyl,*} \approx 1.8\,\text{ms}$ (for the first three sweeps) and for $R_0 \approx 2\,\text{cm}$ in 1.2 ms almost independently of the initial gas pressure in them. According to figure 2, the estimations obtained are rather good ones. Some exceeding the experimental data appears to be due to a portion of the energy of external explosive load being consumed to supply rotational kinetic energy (per unit length) to the fluid filling the cavity as it collapses.

Equation (2.3) can be integrated to obtain the expression for the radial velocity of the cavity, which allows a simple estimation for the compression ratio to be deduced assuming that $R_0/R \gg 1$ (when $\dot{R} \to 0$):

$$\left(\frac{R_0}{R_{min}} \right)^{2\gamma - 3/2} \approx \left(\tfrac{4}{3}\gamma - 1 \right) \bar{p}^{-1}.$$

A calculation using this relation gives the following results for the compression ratio: $R_0/R_{min} \approx 5.3$, 12.2, 21 and 31 for $p_0 = 60$, 20, 10 and 6 kPa, respectively. For the first, second and third values the agreement with the experiment is satisfactory: we have 6, 12 and 20, respectively. Estimating the experimental value of R_{min} for the fourth case (and comparing it with theoretical data) is found to be impossible because of the complicated shape of the sweep in the vicinity of a minimum radius.

3. Axisymmetric collapse of a rotating shell (experiment)

The second schematic of the experiment is presented in figure (3*a*), which shows the principal experimental block comprising the 'transparent tank 1 and piston 2. The high-voltage and recording part of this experimental set-up is the same as that described in § 2.1. Unlike the first set-up (figure 1) wherein the main experimental

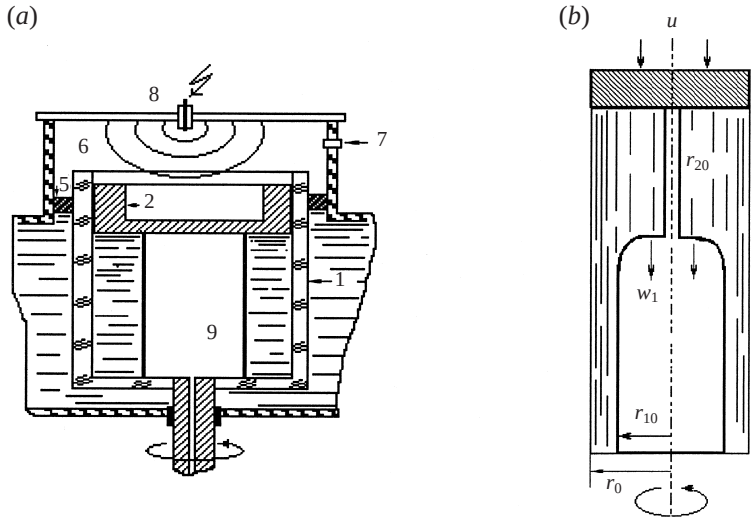

FIGURE 3. (*a*) Device for the study of the cavity motion in a rotating fluid under pulse changes of its height. (*b*) The bore at the surface of the cavity: u and w_1 are velocities of the piston and the bore, r_{10} and r_{20} are the cavity radii before and after the jump.

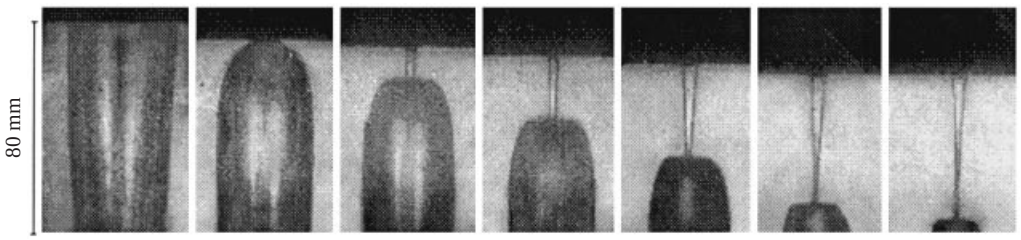

FIGURE 4. Formation of a bore at the cavity surface; the frames (from left to right) correspond to the instants of time of 0, 0.8, 1.2, 1.6, 2.0, 2.4 and 2.6 ms.

block is the transparent tank 1, inner cup 2 and annular piston 3, the inner cup is absent and piston 2 occupies the whole cross-section of the transparent tank 1. A high-speed camera HS-cam operates within the frame regime.

An explosion of the mixture in the high-pressure chamber 6 in this case considerably changes the conditions of compression of the cylindrical cavity 9 formed between the piston 2 and the bottom of the transparent tank 1. In fact, in this set-up, the dynamics of the cavity under axial loading is studied, when the height of the rotating cylindrical shell dynamically varies almost instantaneously over its entire section.

Characteristic frames from the high-speed photography of the flow-development process are presented in figure 4, and a schematic showing the basic parameters of the axisymmetric flow is given in figure 3(*b*) wherein the transparent tank 1 with piston 2 is scale-magnified. A dark line in the upper part of the frames in figure 4 denotes the piston moving from the top down. It was found that in this set-up the cavity collapses suddenly, if the fluid is assumed as practically incompressible, followed by the formation of a jump (bore) (Kedrinskii & Pigolkin 1964).

The process of cavity collapse occurs solely near the piston ($t = 0.8$ ms), along its surface, and continues up to some limit, first forming a characteristic 'neck' ($t = 1.2$ ms in figure 4, of radius r_{20} see figure 3*b*) in the portion of the gas cavity adjacent to

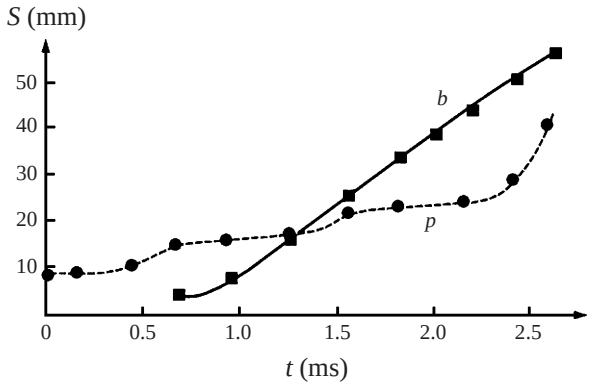

FIGURE 5. Dynamics of basic characteristics of bore formation: curves p and b are displacements of the piston and bore, respectively.

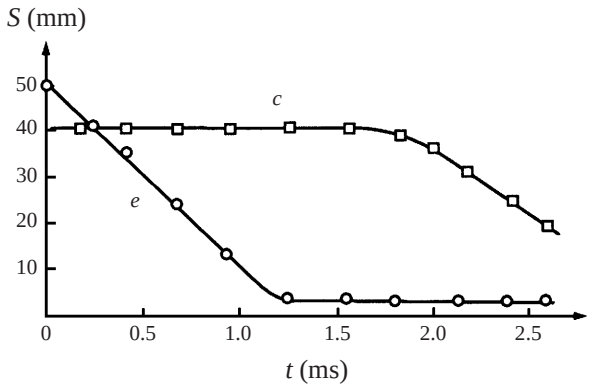

FIGURE 6. Dynamics of basic characteristics of bore formation: change in the cavity diameter near the tank bottom c and average 'neck' diameter of the cavity after the jump e.

the piston. Note that this limit obviously cannot be determined by the gas-pressure change inside the cavity, the bulk of which still retains practically its initial magnitude and is connected with the 'neck'. One can assume that upon forming the 'neck' in the vicinity of the piston, the formation of the jump (bore) is practically accomplished and the subsequent transformation of the cavity shape occurs essentially in the axial direction as a result of this bore propagation.

As previously mentioned, the instantaneous flow pattern is represented schematically in figure 3(b), where u and w_1 are velocities of the piston and bore, r_{10} and r_{20} are the cavity radii before and after the jump, respectively, and r_0 is the cylinder radius.

The bore-forming process is conveniently followed from the dynamics of its separate characteristics presented in figures 5 and 6. Displacement of the piston is shown as curve p (figure 5) pointing to the tendency for an increase of its average velocity whose magnitude in the time interval 1.2–2.4 ms can be estimated as $\bar{u} \approx 10\,\mathrm{m\,s^{-1}}$. The modulation of the function $p(t)$ by low-frequency oscillations is explained by consecutive reflections of the detonation and thus shock waves from the walls and piston in section 6 (figure 3a).

The curve e showing the formation of the 'neck' (figure 6), demonstrates that the jump in the experiments discussed above is completely formed by the moment

$t \approx 1.2$–1.3 ms. From this time on, the average neck diameter is essentially unchanged (the curve e becomes horizontal). Even at $t \approx 1$ ms the bore has become stationary (curve b in figure 5) and propagates with a near-constant velocity of $w_1 \approx 32.6\,\mathrm{m\,s^{-1}}$. Curve c (figure 6) shows the diameter dynamics of the rotating cylindrical cavity ($2r_{10}$, figure 3b, before a jump) near the tank bottom. It is easy to see that, beginning at about $t \approx 1.6$–1.7 ms, the flow becomes two-dimensional: the cavity collapses intensively both along the radius and along the axis. Note that thereafter the intense cavity collapse starting shortly (curve c in figure 6) before the jump does not affect its velocity even though the cavity collapse becomes two-dimensional because the change of the condition before the jump is added.

For comparison with the results of the theoretical analysis given below for the bore shape, it is helpful to know the following two parameters: (a) the ratio δ_d of the initial cavity diameter before the jump to its diameter after the jump ('neck' diameter, $2r_{20}$) and (b) the ratio of velocities in the 'bore–piston' system. For the experimental conditions shown in figure 4 (the height of the cavity $h \approx 80$ mm and diameter $2r_{10} \approx 40$ mm) the ratio δ_d is approximately equal to 10. Note that despite the decrease of the cavity diameter before the jump, according to the experimental data the quantity δ_d remains practically constant at least until time 2.5 ms, close to the complete collapse of the cavity. The ratio of the bore w_1 and piston u velocities is about 3.3.

Experiments with a relatively wide cavity ($h/r_{10} \approx 0.25$) showed that the bore effect holds. In this case $\delta_d \approx 2.6$ and the above ratio of velocities is about 1.8.

4. Theoretical model of a bore in a rotating fluid

In the construction of the theory we assume that an abrupt change in the cavity radius is analogous in nature to a hydraulic jump or bore, travelling over the surface of shallow water. We shall describe the jump motion within the ideal-fluid framework in the long-wavelength (along the rotation axis) approximation. Theoretically, the bore in this case is a place where the flow parameters change from their values before the jump to new values after the jump. This is also true for the flow velocity, streamline positions and the cavity radius. Thus the goal of the theory is to find conditions linking the parameters of the flow before and after the jump and to determine the velocity of the discontinuous motion.

First a general theory of the jump motion along the axis of a hollow vortex is constructed. Rigorous results are obtained for the case when only one vorticity component is non-zero – the azimuthal one. This implies, for instance, that velocity circulation around the axis is constant throughout the flow. Further, the results of the general theory are compared with the experiment. Although in the experiment the velocity circulation around the axis is not constant, because the fluid is in solid-body rotation, it is expected that the theory can predict the velocity of the bore motion and cavity radius after the jump, given the piston velocity, initial cavity radius and characteristic value of the velocity circulation around the axis.

4.1. *Formulation of the problem; derivation of basic equations*

Consider a rotationally symmetric flow of an ideal incompressible fluid in a circular cylinder. The gravity force is neglected. Let us introduce a cylindrical coordinate system $(\tilde{r}, \phi, \tilde{z})$, where $\tilde{r}$ is the radius and the $\tilde{z}$-axis is directed along the axis of symmetry. The fluid occupies the domain $r_1(\tilde{z}, \tilde{t}) \leqslant \tilde{r} \leqslant r_0$, where r_0 is the constant radius of the cylinder and $r_1(\tilde{z}, \tilde{t})$ is the radius of the free surface, $\tilde{t}$ is the time.

Let (u_r, u_ϕ, u_z) denote the velocity components corresponding to $(\tilde{r}, \phi, \tilde{z})$; $\tilde{p}$, $\tilde{\rho}$ are the pressure and density. Futher, Euler's equation will be considered in the long-wave approximation. The following boundary conditions are assumed: $u_r = 0$ at the cylinder boundary ($\tilde{r} = r_0$) and

$$\tilde{p} = 0, \qquad u_r = \frac{\partial r_1}{\partial \tilde{t}} + u_z \frac{\partial r_1}{\partial \tilde{z}}$$

at the free surface ($\tilde{r} = r_1(\tilde{z}, \tilde{t})$).

In order to proceed to the long-wave approximation, unit scales of length, velocity and density are introduced: L is the characteristic scale of changes along the $\tilde{z}$-axis, v_0 is the characteristic value of the rotational velocity component at the boundary of the cavity (for instance, at $\tilde{z} = 0$, $\tilde{t} = 0$, $\tilde{r} = r_1$) and $\tilde{\rho}$ is the density. Using these scales, dimensionless values of η, z, t, q, A, w, p are introduced according to relations

$$\tilde{r}^2 = \eta\delta^2 L^2, \quad \tilde{z} = zL, \quad \tilde{t} = tL/v_0, \quad 2u_r\tilde{r} = q\delta^2 v_0 L, \quad u_\phi \tilde{r} = A\delta v_0 L,$$

$$u_z = wv_0, \quad \tilde{p} = p\tilde{\rho}v_0^2, \quad \rho = \tilde{\rho}/\tilde{\rho} = 1.$$

Here $\delta = r_0/L$ is the dimensionless value of r_0. The value $\eta = \eta_1$ corresponds to $\tilde{r} = r_1$ and $\eta = 1$ corresponds to $\tilde{r} = r_0$. Hereafter all quantities are taken in dimensionless form, unless otherwise specified.

For dimensionless values, the equations of motion and continuity with regard to rotational symmetry take the form

$$\left.\begin{aligned} (\delta^2/2)(q_t + qq_\eta - q^2/(2\eta) + wq_z) - A^2/\eta = -2\eta p_\eta, \\ A_t + qA_\eta + wA_z = 0, \\ w_t + qw_\eta + ww_z = -p_z,\ q_\eta + w_z = 0. \end{aligned}\right\} \tag{4.1}$$

Subscripts written in terms of independent variables denote corresponding partial derivatives. The boundary conditions take the form

$$p = 0, \quad q = \eta_{1t} + w\eta_{1z}, \quad \eta = \eta_1, \tag{4.2}$$

$$q = 0, \quad \eta = 1. \tag{4.3}$$

It is assumed that $\delta \ll 1$. Taking the long-wave-limit approximation the terms in (4.1) proportional to δ^2 are omitted. The system obtained is transformed by transition to mixed Euler–Lagrange variables z', t', v, $v \in [0, 1]$ (Teshukov 1991, 1995; Nikulin 1992*a*, Benney 1973), satisfying the relations

$$z' = z, \quad t' = t, \quad \eta = R(z', t', v).$$

Here R satisfies the equation

$$R_{t'} + wR_{z'} = q, \tag{4.4}$$

and initial and boundary conditions

$$R(z', 0, v) = 1 - v(1 - \eta_1(z', 0)), \quad R(z', t', 0) = 1, \quad R(z', t', 1) = \eta_1(z', t');$$

$\eta_1(z', 0)$ is the given shape of the free surface at $t' = 0$, and $\eta_1(z', t')$ is the unknown shape of the free surface at the moment t'.

It is easy to see that given this definition of R, the boundary conditions (4.2) (for q) and (4.3) are satisfied automatically. In doing this the unknown boundary $\eta = \eta_1(z', t')$ is transformed into the known one $v = 1$. The boundary $\eta = 1$ is transformed into $v = 0$.

For differentiation operators one may write

$$\frac{\partial R}{\partial v}\frac{\partial}{\partial z} = \frac{\partial R}{\partial v}\frac{\partial}{\partial z'} - \frac{\partial R}{\partial z'}\frac{\partial}{\partial v}, \quad \frac{\partial R}{\partial v}\frac{\partial}{\partial \eta} = \frac{\partial}{\partial v},$$

$$\frac{\partial R}{\partial v}\frac{\partial}{\partial t} = \frac{\partial R}{\partial v}\frac{\partial}{\partial t'} - \frac{\partial R}{\partial t'}\frac{\partial}{\partial v}.$$

Then in z', t', v variables, after omitting the terms with δ^2, the system (4.1) in view of (4.4) takes the form (hereafter the primes on z', t' are omitted)

$$A^2/(2R^2)R_v = p_v, \tag{4.5a}$$

$$A_t + wA_z = 0, \tag{4.5b}$$

$$R_v(w_t + ww_z) = -R_v p_z + R_z p_v, \tag{4.5c}$$

$$R_{vt} + (wR_v)_z = 0. \tag{4.5d}$$

Next, conditions at the discontinuity are formulated and solvability of the equations following from them is proved. For shallow water similar conditions were formulated and analysed by Teshukov (1995).

4.2. *Conditions at the discontinuity*

It follows from the definition of v and R that v is the number of a liquid streamline and R is the ratio of the square of the radial distance from the axis to the liquid streamline with a given v at fixed z and t, to the cylinder radius squared. Consider that at transitions across the discontinuity the liquid streamlines retain their individuality, i.e. to each streamline before the discontinuity these corresponds a steamline after the discontinuity. The radial distance to the axis for the given liquid streamline, axial velocity and some other parameters of the flow will change abruptly at transition across the discontinuity. Then for each value of v there will be two corresponding values of the same parameter before and after the discontinuity. Thus the conditions at the discontinuity must link the values of corresponding parameters at each v before and after the discontinuity.

In order to obtain the conditions at the discontinuity it is necessary to put equations (4.5) into a divergent form and, considering their physical meaning, define which quantities have a jump discontinuity and which do not. The difference of the quantities before and after the discontinuity is denoted by square brackets. From (4.5*d*) which already has a divergent form, we obtain for this difference $[R_v(w-D)]$, where D is the velocity of the front motion. The physical meaning of this expression is the following. The quantity $R_v\mathrm{d}v$ is (in dimensionless form) the element of an annular area bounded by the liquid streamlines with coordinates v and $v+\mathrm{d}v$. Then $R_v(w-D)\mathrm{d}v$ is the mass flow in the annular tube of flow with area $R_v\mathrm{d}v$ in the system of reference associated with the discontinuity front. Assume that at transition across the discontinuity the mass flow along the tube is conserved. Then the condition (4.5*d*) takes the form

$$[R_v(w - D)] = 0. \tag{4.6}$$

Equation (4.5*b*) after multiplying it by R_v, in view of (4.5*d*), takes the divergent form

$$(R_v A)_t + (wR_v A)_z = 0,$$

which allows, assuming (4.6), determination of the expression for the jump in the

form

$$[R_v(w-D)A] = [A](R_v(w-D)).$$

Thus it follows that the velocity circulation on the liquid streamline may be conserved at transition across the jump. Assuming that this is valid, we obtain the second condition at the discontinuity

$$[A] = 0, \tag{4.7}$$

which allows simplification of the problem. In the case of continuous motion both the original system (4.1) and its long-wave approximation have a solution with $A = \text{const}$. Assume that in the flow before discontinuity $A = \text{const}$. By virtue of (4.7) this condition is not violated at the discontinuity either. Thus the system (4.5) with $A = \text{const}$ has a solution throughout the entire flow domain (both before and after the discontinuity) which enables us to set

$$A = \text{const} \tag{4.8}$$

and simplify the system (4.5), in which p is excluded by integrating (4.5a) over v, and taking into account that $p = 0$ at $v = 1$. As a result, two equations remain

$$w_t + ww_z + (A^2/2)(R_0^{-1})_z = 0, \tag{4.9a}$$

$$R_{vt} + (wR_v)_z = 0, \tag{4.9b}$$

where R_0 is the value of R at $v = 1$. From this, switching to the frame of reference associated with the jump, and assuming that the flow in it is stationary, we obtain the expression

$$((w-D)^2/2 + A^2(2R_0)^{-1})_z = 0.$$

According to (4.5a)

$$A^2(2R_0)^{-1} = p + A^2(2R)^{-1} = p + v^2/2,$$

where v is the rotational velocity component. Thus the expression obtained represents the derivative of the total head with respect to z in the reference system, related to the jump, in the long-wavelength approximation. It is not reasonable to consider that the total head is conserved at transition across the discontinuity, because the energy may dissipate or transform from the average motion into the energy of short-wavelength oscillations. Therefore we make the following assumptions: (i) the total head along a streamline may decrease at transition across the jump; (ii) if the total head decreases, it changes by the same value on each line of flow. The latter assumption is heuristic in character and must be supported by agreement of the theoretical estimations wih experimental data.

Then the third condition at the jump takes the form

$$[w(w-2D) + A^2R_0^{-1}] = K\,, \tag{4.10}$$

where $K \leqslant 0$ (if the parameters before the jump are subtracted from the parameters after the jump) and K does not depend on v ($K_v = 0$). Note that the latter condition can be obtained by other means.

In rotationally symmetric flows with $A = \text{const}$ another quantity appears – the azimuthal vorticity component divided by radius – which is conserved in the course of motion in a liquid particle by virtue of the original equations (4.1). In dimensionless variables it has the form

$$(\omega\eta^{-1/2}) = -w_\eta + q_z\delta^2/(4\eta).$$

Passing to the long-wavelength approximation and z, v variables, we obtain for α the expression

$$\alpha = (\omega\eta^{-1/2}) = -w_v(R_v)^{-1}$$

and the equation in divergent form

$$(\alpha R_v)_t + (wR_v\alpha)_z = 0,$$

whence, in view of (4.6), follows the expression for the jump

$$[R_v(w-D)\alpha] = [\alpha](R_v(w-D)).$$

Assume that neither α, nor A, experiences the discontinuity, which results in the condition

$$[w_v(R_v)^{-1}] = 0. \tag{4.11}$$

In turn, from (4.10), in view of (4.6) it follows that

$$K_v = [2w_v(w-D)] = [2w_vR_v^{-1}].$$

Then according to (4.11) we obtain $K_v = 0$ and thus by virtue of (4.11), K does not depend on v: the change of the total head is the same for all streamlines. Note that the condition $K_v = 0$ was derived by Teshukov (1995) for a plane flow of shallow water under the assumption that at the jump, the circulation is conserved along a streamline.

Assume that the value of A is given. Then, if K in (4.10) is known, relations (4.6) and (4.10) would be sufficient for determination of the jump parameters. However, the losses of the total head at the jump are unknown, therefore the value of K is not determined and must be found from the solution. Consequently, one more relation is required, for which an integral law of conservation of the 'flow force' is taken.

For a smooth cylinder this assumption is quite natural. The 'flow force' is obtained from (4.9*a*) after its multiplication by R_v and integration over v from 0 to 1. As a result, in view of (4.9*b*) and that $R = 1$ at $v = 0$, we obtain the condition at the jump:

$$\left[\int_0^1 R_v w(w-D)\mathrm{d}v - \tfrac{1}{2}A^2(\ln R_0 + R_0^{-1})\right] = 0. \tag{4.12}$$

Below we shall prove that given the parameters of the flow before the discontinuity ($w(v)$, $R(v)$) and either D or one of the functions w or R after it, relations (4.6), (4.10), (4.12) completely define the jump. The constant K is also found from the solution.

4.3. *Solvability of conditions at the discontinuity*

Without loss of generality, consider relations (4.6), (4.10), (4.12) in a reference frame related to the front. In this case one should set $D = 0$, and w now means the velocity relative to the front. Let the parameters before the discontinuity in the reference frame of the front be given: $w_1(v)$, $R_1(v)$. It is assumed that $w_1 \geqslant \gamma > 0$, $R_1(v) = 1-v(1-R_{10})$, where R_{10} is the value of R_1 at $v = 1$. This form of $R_1(v)$ obviously does not restrict the generality of considerations, since we may choose any convenient way of numbering the streamlines before the discontinuity. Consider the problem of the determination

of the parameters after the front, $w_2(v)$, $R_2(v)$. Let us introduce the notation

$$\left.\begin{aligned} \psi &= w_2^2 - w_1^2, \\ F(\psi) &= \psi + A^2(-R_{10}^{-1} + R_{20}^{-1}), \\ E(\psi) &= \int_0^1 (1 - R_{10}) w_1 [(w_1^2 + \psi)^{1/2} - w_1] \mathrm{d}v + \tfrac{1}{2} A^2 (\ln R_{20} + R_{20}^{-1} - \ln R_{10} - R_{10}^{-1}). \end{aligned}\right\} \tag{4.13}$$

Here R_{20} is the value of R_2 at $v = 1$, and ψ is a new unknown function (instead of w_2). Since $w_1 \geqslant \gamma > 0$, for definiteness of the square-root expression we set $\psi \geqslant -\gamma^2$, which corresponds to $w_2 \geqslant 0$. Then (4.6), (4.10), (4.12), in view of $D = 0$ and expressions for $R_1(v)$, w_2, take the form

$$(1 - R_{10}) w_1 + R_{2v}(w_1^2 + \psi)^{1/2} = 0, \tag{4.14}$$

$$F(\psi) = K \leqslant 0, \tag{4.15}$$

$$E(\psi) = 0. \tag{4.16}$$

From (4.14) one may find R_{20}

$$R_{20} = 1 - \int_0^1 w_1 (1 - R_{10})(w_1^2 + \psi)^{-1/2} \mathrm{d}v. \tag{4.17}$$

Since $K = \text{const}$, from (4.15) it follows that ψ does not depend on v and the possibility arises of considering it as a new independent variable. Thus the problem reduces to finding the non-trivial solution of (4.16), (4.17) with the condition (4.15). After obtaining ψ, one can then determine w_2, R_2 and K from (4.13)–(4.15).

Let us determine the conditions under which a solution of the system (4.15)–(4.17) exists. Let

$$\lambda = \frac{(1 - R_{10}) A^2}{2 R_{10}^2} \int_0^1 \frac{\mathrm{d}v}{w_1^2}. \tag{4.18}$$

Then the following statements are true.

If $\lambda < 1$, the system (4.15)–(4.17) has a solution, and if $E(-\gamma^2) \geqslant 0$, the solution is unique. If $\lambda > 1$, a solution does not exist.

1. Let $\lambda < 1$. Differentiating $F(\psi)$, $E(\psi)$ we have:

$$F''(\psi) > 0, \; F'(0) = 1 - \lambda, \quad 2E'(\psi) = (1 - R_{20}) F'(\psi). \tag{4.19}$$

These relations follow from the definitions of $F(\psi)$, $E(\psi)$, R_{20} and the easily verified inequality $R_{20}'' < 0$. Since $F''(\psi) > 0$, $F'(\psi)$ monotonically increases, and $F(\psi)$ is a function convex downwards. From the expression for $F'(0)$ it follows that for $\lambda < 1$, $F'(0) > 0$. Then $F'(\psi) > 0$ for $\psi > 0$. Since $1 - R_{20} > 0$, from (4.19) it follows that the sign of $E'(\psi)$ is the same as the sign of $F'(\psi)$. Consequently, in this case $E'(\psi) > 0$ for $\psi > 0$. Because $E(0) = 0$, $E(\psi) > 0$ for $\psi > 0$. From this $E(\psi)$ can become zero only for $\psi < 0$. Let $E(-\gamma^2) \geqslant 0$. Then owing to $E'(\psi)$ and $F'(\psi)$ having the same sign, the monotonic decrease of $F'(\psi)$ as ψ decreases from 0 to $-\gamma^2$ and inequality $F'(0) > 0$, the function $E(\psi)$ first decreases to some minimum value and then increases constantly as ψ changes from 0 to $-\gamma^2$. Therefore, if $E(-\gamma^2) \geqslant 0$, a unique value of $\psi_1 < 0$ necessarily exists, such that $E(\psi_1) = 0$. Let us now find the sign of $F(\psi_1)$. If $F(\psi_1) \leqslant 0$, then $\psi = \psi_1$ will be a solution of the system (4.15)–(4.17). Suppose that

$F(\psi_1) > 0$. Then by virtue of the properties of the function $F(\psi)$, a ψ_2, $\psi_1 \leqslant \psi_2 < 0$, can be found such that $F(\psi_2) = 0$. Then, the properties of $E(\psi)$ imply the inequality $E(\psi_2) < 0$. Integration of (4.19) from ψ_2 to 0 yields

$$-2E(\psi_2) = \int_{\psi_2}^{0} R'_{20} F(\psi) \mathrm{d}\psi. \tag{4.20}$$

It can be easily verified that $R'_{20} > 0$. Obviously, $F(\psi) < 0$ for $\psi_2 < \psi < 0$. Then the right-hand side of (4.20) is less than zero, and the left-hand side is greater than zero.

The contradiction obtained proves that the assumption $F(\psi_1) > 0$ is wrong. Thus, $F(\psi_1) \leqslant 0$ and a solution for $\lambda < 1$ exists and is unique if $E(-\gamma^2) \geqslant 0$.

If $E(-\gamma^2) < 0$, a solution can be constructed in the following manner. Assume that after the jump, in the region where R_2 changes from $R_{20}(-\gamma^2)$ to some $\Delta < R_{20}(-\gamma^2)$ to be found in the course of the solution, a stagnant zone originates in which the fluid has zero axial velocity but rotates with constant circulation. From the mathematical standpoint this leads to a change of the relations at the transition. In this case in (4.15), (4.16) one should put $\psi = -\gamma^2$, and write $R_{20}(-\gamma^2) - \Delta$ instead of R_{20}. Then, similarly to the previous case, it can be proved that some $\Delta > 0$ exists such that $E(\Delta) = 0$, $F(\Delta) < 0$. That is, from the mathematical viewpoint, such a solution is possible. From the physical viewpoint the formation of stagnation zones after the jump is also possible. Note that a similar viewpoint was suggested in the consideration of hydraulic jumps on shallow water by Teshukov (1995).

2. Let $\lambda > 1$. Let us prove that in this case a solution does not exist, i.e. that the jump is impossible under the given assumptions. If $\lambda > 1$, then in view of (4.19), $F'(0) < 0$. This implies that $F'(\psi) < 0$, $E'(\psi) < 0$ for $\psi < 0$. Then $E(\psi)$ cannot become zero for $\psi < 0$. Let there be some $\psi_1 > 0$ such that $E(\psi_1) = 0$. Let us find the sign of $F(\psi_1)$. Suppose that $F(\psi_1) \leqslant 0$. Then by virtue of the properties of function $F(\psi)$ and $E(\psi)$, there exists some $\psi_2 \geqslant \psi_1$ such that $F(\psi_2) = 0$, $E(\psi_2) > 0$ (since the sign of $E'(\psi)$ is the same as the sign of $F'(\psi)$, and for $\psi > \psi_1$ it is apparently positive). Upon integrating (4.19) from 0 to ψ_2 we obtain

$$2E(\psi_2) = \int_{0}^{\psi_2} R'_{20} F(\psi) \mathrm{d}\psi. \tag{4.21}$$

From the properties of $F(\psi)$ on the interval $(0, \psi_2)$, $F(\psi) < 0$. Since $R'_{20} > 0$, the right-hand side of (4.21) is negative, whereas the left-hand side is positive. The contradiction obtained proves that the inequality $F(\psi_1) \leqslant 0$ does not hold. Thus at $\lambda > 1$ there is no transition satisfying (4.15). Since from physical considerations it is evident that the total head cannot increase at transition across the jump, then for $\lambda > 1$, under the assumptions made, the jump is impossible.

Let us discuss the meaning of conditions $\lambda > 1$, $\lambda < 1$. For $A = \text{const}$ the long-wave approximation equations (4.9) are similar to those of vortex a shallow in water, Teshukov (1991). The difference between them is that gravitational acceleration g is replaced by centrifugal acceleration $A^2/(2R_0^2)$. Then the equation obtained in Benney (1973) and Teshukov (1991), after an appropriate modification, can be used to determine the velocity of propagation of the free surface perturbation. With this method Nikulin (1994) showed that condition $\lambda = 1$ corresponds to the fact that the velocity of an infinitesimal perturbation is zero relative to a coordinate system fixed in space. Then it is easily seen that the condition $\lambda < 1$ implies that the velocity of an infinitesimal perturbation is greater than zero. Hence any infinitesimal perturbation will be transported downstream. If $\lambda > 1$ the opposite situation takes place. So, in

the problem considered the parameter $1/\lambda$ plays the role of the Froude number for shallow water flow. Therefore the flow with $\lambda < 1$ can be called supercritical and that with $\lambda > 1$ subcritical. Consequently, under the assumptions made, the jump is possible only at transition from a supercritical state to a subcritical one.

From the statements proved a corollary follows. The cavity radius after the jump is always smaller than before the jump, i.e. $R_{20} < R_{10}$. Let us prove it. It was found that a solution exists if $\lambda < 1$. In this case, $\psi < 0$ after the jump. Since $R_{20}(0) = R_{10}$, $R'_{20}(\psi) > 0$, then $R_{20}(\psi) < R_{10}$ for $\psi < 0$.

4.4. *Comparison with experiment*

Let us apply the results of the general theory to a description of the experiments. In the experiments the flow in an unperturbed state was in solid-body rotation, therefore its circulation around the axis depended on r. However, if the circulation varies moderately, the model must describe qualitative mechanisms and, in order of magnitude, quantitative experimental results as well. In comparing the results we consider the cavity radius before the front r_{10} and the velocity of the piston motion $\tilde{u}$ as given values. The cavity radius after the jump r_{20} and the velocity of the front motion $\tilde{D}$ will be calculated. As a typical velocity we take the value of the rotational velocity component at the cavity boundary in the unperturbed state v_0. Here r_{10}, r_{20}, $\tilde{u}$, $\tilde{D}$, v_0 are the dimensional quantities, then the dimensionless quantities are defined as $R_{10} = (r_{10}/r_0)^2$, $R_{20} = (r_{20}/r_0)^2$, $u = \tilde{u}/v_0$, $D = \tilde{D}/v_0$, $A = r_{10}/r_0$ and r_0 is the cylinder radius.

Since in the experiments the jump travels over the fluid, which has zero velocity, then in the reference frame associated with the jump we have $w_1 = D$, $w_2 = w_1 - u$. Assuming that w_1 and u do not depend on v, let us compute the integrals in (4.16), (4.17). Denoting $x = R_{10}/R_{20}$, we obtain

$$\left.\begin{aligned} w_1 &= u(x - R_{10})/[R_{10}(x-1)], \\ A^2(x-1) - 2R_{10}(1-R_{10})w_1 u &= A^2 R_{10} \ln x. \end{aligned}\right\} \tag{4.22}$$

It is easily seen that these equations have a unique solution x and w_1 for given R_{10}, u and A. Let us use their solution for comparison with the experiment.

In the first experiment we have $r_0 = 40\,\text{mm}$, $r_{10} \approx 20\,\text{mm}$, $v_0 \approx 4\,\text{m s}^{-1}$, $\tilde{u} \approx 10\,\text{m s}^{-1}$. Then $u \approx 2.5$, $R_{10} \approx 0.25$, $A \approx 0.5$. Calculation according to (4.22) gives $w_1/u \approx 4$ and $x \approx 40$. The experimental values are equal respectively to $w_1/u \approx 3.3$ and $x \approx 100$.

In the second experiment $r_0 = 40\,\text{mm}$, $r_{10} \approx 30\,\text{mm}$, $v_0 \approx 6\,\text{m s}^{-1}$, $\tilde{u} \approx 10\,\text{m s}^{-1}$. Then $u \approx 1.66$, $R_{10} \approx 0.57$, $A \approx 0.75$. The theoretical results give $w_1/u \approx 1.9$ and $x \approx 5.7$. The experimental values are $w_1/u \approx 1.8$ and $x \approx 6.76$.

Let us calculate the value of the parameter λ. Assuming that w_1 does not depend on v, from (4.16) we find $\lambda = (1 - R_{10})A^2/(2R_{10}^2 w_1^2)$. From this it is easy to verify that under the experimental conditions the inequality $\lambda < 1$ was satisfied.

So, theoretical results agree with experimental observations. Some discrepancy between the experimental and theoretical results is explained by the dependence of the parameter A on r which is not considered by the model. The difference in values of R_{10}/R_{20} in the first series of experiments is due to the fact that for a fast rotating cylindrical shell it is more difficult to eliminate completely a taper. In addition, an increase in the thickness of the liquid shell may lead to a change in the parameter A. Qualitatively, the behaviour of the cavity radius and the value of the parameter λ are found to be comparable.

5. Conclusion

The flow stability has been investigated experimentally when a rotating cylindrical shell is radially converging as a result of its compression by a ring piston under an explosive load. An interface shape asymmetry has been proved to occur in all the cases as a result of liquid rotation. Apart from this effect one can observe some kind of 'twist' of the diameter (more clear-cut on the third frame of figure 2*a*, for $p_0 = 0.1$ atm) and the rather long weak pulsations of a cavity after its first collapse (fourth frame, $p_0 = 0.06$ atm, $t > 2.75$ ms).

The approximate equation of cylindrical cavity dynamics (2.2) has been converted to the corresponding version for an incompressible liquid, (2.3), as a limit transition in sound velocity ($c_0 \to \infty$). Then (2.3) has been used to estimate the main parameters of the cavity dynamics in a rotating liquid (time of collapse and compression ratio). The comparison of the theoretical estimations with the experimental data both in the case of a cylindrical charge explosion and in the case of rotating liquid shell collapse has confirmed the validity of the mathematical model suggested.

We can also conclude that the theoretical bore model is able to describe adequately a stationary bore in a rotating fluid and to provide a qualitative and quantitative estimation for experimental conditions with limited sizes of flow domain.

Assistance from referees in improving the presentation of this work is gratefully acknowledged.

REFERENCES

Atchley, A. A. 1993 Review of recent advances in synchronous picosecond sonoluminescence. In *Proc. 13th Intl Symp. on Nonlinear Acoustics, Bergen* (ed. H. Hobaek), pp. 36–42. World Scientific.

Benjamin, T. B. 1962 Theory of the vortex breakdown phenomenon. *J. Fluid Mech.* **4**, 593–629.

Benney, D. J. 1973 Some properties of long nonlinear waves. *Stud. Appl. Maths* **52**, 45–50.

Besant, W. H. 1859 *Hydrostatics and Hydrodynamics*, Art. 158. Cambridge University Press.

Book, D. & Lohner, R. 1989 Quatre foil instability of imploding cylindrical shock. In *Proc. Intl Workshop on Shock Wave Focusing, Sendai* (ed. K. Takayama), pp. 193–206. Tohoku University.

Cole, R. 1948 *Underwater Explosions*. Princeton University Press.

Crum, L. A. 1994 Sonoluminescence. *Physics Today*, Sept, 22–29.

Demmig, F., Gronig, H., Kleine, H. & Wallus, H. 1993 Experiments and model computation of cylindrical shock waves with time-resolved deformation and fragmentation. In *Proc. 19th Intl Symp. on Shock Waves*, *July 26–30, Marseille* (ed. R. Brun & L. Z. Dumitrescu), vol. 4, pp. 87–92.

Fujiwara, K., Matsuo, H. & Hiroe, T. 1993 New methods for generating cylindrical imploding shock. In *Proc. 19th Intl Symp. on Shock Waves*, *July 26–30, Marseille* (ed. R. Brun & L. Z. Dumitrescu), vol. 4, pp. 81–86.

Gaitan, D. F. & Crum, L. A. 1990 Observation of sonoluminescence from a single, stable cavitation bubble in a water–glycerine mixture. In *Proc. 12th Intl Symp. on Nonlinear Acoustics, Austin* (ed. M. Hamilton & D. Blackstock), pp. 459–463. Elsevier.

Gronig, H. 1989 Past, present and future of shock focusing research. In *Proc. Intl Workshop on Shock Wave Focusing, Sendia* (ed. K. Takayama), pp. 1–38, Tohoku University.

Hiroe, T., Matsuo, H. & Fujiwara, K. 1993 A numerical study of explosive-driven cylindrical imploding shocks in solids. In *Proc. 19th Intl Symp. on Shock Waves*, *July 26–30, Marseille* (ed. R. Brun & L. Z. Dumitrescu), vol. 3, pp. 267–272.

Isuzukawa, K. & Horiuchi, M. 1991 Experimental and numerical studies of blast wave focusing in water. In *Proc. 18th Intl Symp. on Shock Waves*, *July 21–26, Sendai*, vol. 1, pp. 347–350.

Kedrinskii, V. K. 1971 In *Proc. of Institute of Hydrodynanics, Dynamics of Continium Medium*, issue 8, pp. (in Russian).

KEDRINSKII, V. K. 1976 Some approximate models for a cylindrical cavity pulsation in an uncompressible liquid. *Combustion, Explosion and Shock Waves* (translated from Russian to English by Plenum Publishing Corporation), No. 5, 768–773.

KEDRINSKII, V. K. & KUZAVOV V. T. 1977 Dynamics of cylindrical cavity in a compressible fluid. *Appl. Mech. Tech. Phys.* (translated from Russian to English by Plenum Publishing Corporation), No. 4, 102–106.

KEDRINSKII, V. K. & PIGOLKIN G. M. 1964 On the stability of a collapsing gas cavity in a rotating fluid. *Appl. Mech. Tech. Phys.* (translated from Russian to English by Plenum Publishing Corporation), No. 3, 113–117.

KELLER, J. J., EGLI, W. & EXLEY, J. 1985 Force- and loss-free transitions between flow states. *Z. Angew. Math. Phys.* **36**, 856–888.

KUWAHARA, M. *et al.* 1991 The problems of focused shock waves effect on biological tissues. In *Proc. 18th Intl Symp. on Shock Waves*, *July 21–26, Sendai* vol. 1, pp. 41–48.

NIKULIN, V. V. 1992*a* Analogue of the shallow-water vortex equation for hollow and tornado-like vortices. *J. Appl. Mech. Tech. Phys.* No. 2, 47–52.

NIKULIN, V. V. 1992*b* Space evolution of tornado-like vortex core. *Intl Ser. Numer. Maths* **106**, 229–237.

NIKULIN, V. V. 1994 A hollow vortex with an axial velocity in a tube of variable radius. *J. Appl. Math. Mech.* **58**, No. 2, 235–239.

RAYLEIGH, LORD 1917 On the pressure development in a liquid during the collapse of a spherical cavity. *Phil. Mag.* **34**, 94–98.

STURTEVANT, B. 1989 The physics of shock wave focusing in the context of extracorporeal shock wave lithotripsy. In *Proc. Intl Workshop on Shock Wave Focusing, Sendai* (ed. K. Takayama), pp. 39–64. Tohoku University.

TAKAYAMA, K. 1989 High pressure generation by shock wave focusing in ellipsoidal cavity. In *Proc. Intl Workshop on Shock Wave Focusing, Sendai* (ed. K. Takayama), pp. 1–37. Tohoku University.

TARZHANOV, V. I. 1995 Cumulative gas compression geometry intermediate between spherical and cylindrical ones. In *Proc. Intl Conf. IV-th Zababakhin Scientific Talks, October 16–20, Snezhinsk, Russian Federal Centre VNI Institute of Technical Physics*, pp. 44–49.

TESHUKOV, V. M. 1991 Long wave approximation for vortex free boundary flows. *Intl Ser. Numer. Maths* **99**, 413–420.

TESHUKOV, V. M. 1995 Hydraulic jump in the shear flow of an ideal incompressible fluid. *J. Appl. Mech. Tech. Phys.* **31**, No. 1, 10–18.

VAKHRAMEEV, YU. S. 1995 The nature of instability of some convergent flows. In *Proc. Intl Conf. IVth Zababakhin Scientific Talks, October 16–20, Snezhinsk, Russian Federal Centre VNI Institute of Technical Physics*, pp. 1–6.

WHITHAM, C. B. 1974 *Linear and Nonlinear Waves*. Wiley.

ZABABAKHIN, I. E. 1970 Phenomena of unlimited convergence. In *Mechanics in the USSR Over the past 50 Years*, pp. 313–342. Nauka.